Chemical Physics Impact 7 (2023) 100332

Contents lists available at ScienceDirect

Chemical Physics Impact

journal homepage: www.sciencedirect.com/journal/chemical-physics-impact

# Impact of water addition on fluctuation dynamics in viscous solvents with varied heterogeneity: A 2D IR spectroscopic study

Tubai Chowdhury [a,b], Sucheta Ghosh [c], Akhil Pathania [a,b], Shivshankar Kore [a,b], Akhil B Mon [d], Srijan Chatterjee [a,b], Samadhan H. Deshmukh [a,b], Sayan Bagchi [a,b,*]

[a] Physical and Materials Chemistry Division, CSIR-National Chemical Laboratory, Pune 411008, India
[b] Academy of Scientific and Innovative Research (AcSIR), Ghaziabad 201002, India
[c] School of Chemical Sciences, Indian Association for the Cultivation of Science, 2A Raja SC Mullick Road, Kolkata, West Bengal 700032, India
[d] Indian Institute of Science Education and Research (IISER), Mohali, Punjab 140306, India

ARTICLE INFO

*Keywords:*
Solvation dynamics
Ultrafast dynamics
Deep eutectic solvent
Viscosity
2DIR spectroscopy

ABSTRACT

The addition of cosolvent, such as water, influences the overall fluctuation dynamics as sensed by the probe. It is crucial to unravel the fluctuation dynamics when water is added, particularly in viscous solvents with varying degrees of heterogeneity. In this study, we employed two-dimensional infrared spectroscopy to examine the solvation dynamics of two viscous solvents: glycerol, a molecular solvent, and malicine, an acid-based deep eutectic solvent. Additionally, we explored the relative changes in fluctuation dynamics upon water addition. Our results indicate that water disrupts the hydrogen bond network in glycerol, but no significant effect is observed in malicine. Our experimental findings align well with previously reported simulation studies.

## 1. Introduction

Cosolvency refers to the effects of adding one or more solvents (cosolvents) that are different from the existing solvent in a solution on the properties of the solution or the behavior of the solute. Aqueous phase cosolvency, in particular, has found applications in numerous scientific and engineering disciplines [1–4]. In this context, water is a significant portion of the solvent mixture. One of the main advantages of using water as a cosolvent is its ability to significantly reduce the viscosity of the solution, even when the other component is highly viscous [5–7]. For instance, mixing viscous molecular solvents like glycerol ($\eta \sim 1$ Pa s) with water has been widely utilized in various applications [8–11]. An interesting property of these mixtures is their ability to hinder crystallization, making them effective antifreeze components [12–14].

Another application of water as a cosolvent can be found in deep eutectic solvents (DESs), which have garnered attention as promising green alternatives to conventional solvents due to their favorable properties in a wide range of applications [3,15–17]. DESs are typically prepared by mixing a hydrogen bond donor (HBD) and a hydrogen bond acceptor (HBA), leading to an extensive hydrogen bond network as a result of charge delocalization through hydrogen bonding [18,19].

DESs are inherently viscous liquids, and the addition of water reduces the viscosity to facilitate various applications. While acid-based DESs are known to exhibit significantly higher viscosity ($\eta > 1$ Pa s) [20] compared to urea/alcohol based-DESs, most of the previous experimental studies have been limited to the urea/alcohol-based DESs [5,21–24]. Furthermore, unlike molecular solvents like glycerol, DESs are characterized by spatial heterogeneity, forming many domains with different microenvironments [19,25–29]. When a cosolvent like water is added to DESs, the dynamics experienced by solutes trapped in the nanoscopic heterogeneous pockets of the DES can undergo significant changes [5,21,30–32]. In comparison, molecular solvents like glycerol provide a more uniform environment overall for the solute due to the homogeneity of the system [33]. This leads to the question of whether the transition from high to low viscosity upon water addition occurs similarly in both heterogeneous DES systems and homogeneous, highly viscous molecular solvents. As bulk viscosity is believed to manifest in the fluctuation dynamics of the solvent system, it becomes essential to understand the differences in the dynamical behavior between viscous molecular solvents, viscous DESs, and their water-diluted versions [8,10,25,34,35]. Previous studies have utilized two-dimensional infrared (2D IR) spectroscopy to investigate solvent fluctuation dynamics in viscous solvent systems and their aqueous mixtures [5,25,36–42].

* Corresponding author at: Physical and Materials Chemistry Division, CSIR-National Chemical Laboratory, Pune 411008, India.
*E-mail address:* s.bagchi@ncl.res.in (S. Bagchi).

https://doi.org/10.1016/j.chphi.2023.100332
Received 22 July 2023; Received in revised form 18 September 2023; Accepted 3 October 2023
Available online 5 October 2023

However, a systematic study to compare the solvation dynamics of viscous molecular solvents, DESs, and their aqueous mixtures has been lacking until now.

In this work, we employed FTIR and 2D IR spectroscopy on glycerol (η = ~1 Pa s), malicine (an acid-based DES (η > 1 Pa s), and their aqueous solutions to address the aforementioned knowledge gap. The experimental investigation of the impact of water addition on a highly viscous acid-based DES is compared to the effects of adding an equal amount of water to a similarly highly viscous molecular solvent. Ammonium thiocyanate was used as the vibrational probe to study solvent dynamics as $SCN^-$ has a high transition dipole (stronger signal) and long vibrational lifetime, which are needed for enquiring the fluctuation dynamics of viscous liquids at higher waiting times [43–46].

Furthermore, $SCN^-$ is widely used as a vibrational probe to understand different systems like ionic liquids, DES, and electrolytes [5,40,47]. The combination of FTIR and 2D IR results provided insights into the behavior of these viscous solvents with water dilution. Our findings revealed a distinct mechanism operating in the two different viscous solvents upon the addition of water.

## 2. Materials and methods

### 2.1. Materials and synthesis

Choline chloride (ChCl, >98.9 %), ammonium thiocyanate ($NH_4SCN$, >99.9 %), and glycerol (>99.0 %) were all acquired from Sigma-Aldrich. At the same time, DL-malic acid (>98 %) was procured from Alfa Aesar. Except for ChCl, the compounds were used without additional purification steps. ChCl was subjected to vacuum oven drying at 80 °C overnight to remove any trace amounts of water. The deep eutectic solvent (DES) was prepared following a previously published procedure [20,48]. In brief, a 1:1 molar ratio of ChCl and malic acid were combined in a round-bottom flask. The mixture was stirred and heated at approximately 50–60 °C until a clear and homogeneous solution was achieved. Subsequently, the homogeneous solution was allowed to cool to ambient temperature to facilitate further spectroscopic measurements. The Glycerol_10W and Malicine_10W mixtures were prepared by adding 10 moles of water to one mole of glycerol and malicine, respectively. Previous studies have suggested that nanostructures in a different DES are somewhat retained with the addition of up to 10–15 moles of water [5,21,24]. However, another simulation report indicates that adding a similar molar ratio of water to glycerol would disrupt the solvation structure of glycerol [33]. Therefore, we chose to use a 10:1 water-to-solvent ratio (10W) to compare the effects of water addition on glycerol and malicine in terms of solvent fluctuation dynamics.

### 2.2. FTIR spectroscopy

FTIR spectra were acquired using a Bruker Vertex 70 FTIR spectrometer equipped with a demountable cell consisting of two $CaF_2$ windows (3 mm thickness) separated by a 50 μm mylar spacer. $NH_4SCN$ was added to glycerol, glycerol-water mixture (Glycerol_10W), malicine, and malicine-water mixture (Malicine_10W) to achieve a final solute concentration of approximately 50 mM. All FTIR experiments were conducted at room temperature, utilizing ~80 μl of the sample solutions. Subsequently, 2D IR experiments were performed on the same sample solutions, employing the same sample cell used for the FTIR measurements.

### 2.3. 2D IR spectroscopy

In this study, the setup used for 2D IR experiments has been described previously [49]. In summary, an optical parametric amplifier (OPA) was pumped by a Ti:Sapphire oscillator/regenerative amplifier, producing mid-IR pulses at 2050 $cm^{-1}$ (10 μJ) with a pulse width of ~70 fs. These mid-IR pulses were split into a powerful pump beam (80 %) and a weak probe beam (20 %) using a beam splitter in the 2D IR spectrometer. The excitation frequency axis of the 2D IR spectra was obtained by scanning a collinear pair of compressed pump pulses with varying time delays ($\tau$) through a germanium acousto-optic modulator (AOM)-based pulse shaper. The pump and probe pulses, spatially overlapped, were focused onto the sample cell by off-axis parabolic reflectors. By keeping a fixed temporal delay (waiting time, $T_w$) between the pump and probe pulses, the scan of $\tau$ produced the 2D IR signal. The signal was dispersed onto a monochromator (Princeton Instruments) and then detected using a liquid nitrogen-cooled 64-pixel mercury cadmium telluride IR array detector (InfraRed Associates). A series of 2D spectra were collected at various $T_w$ values.

The $T_w$ dependent changes in the 2D spectral shape provided time-dependent information, which was analyzed through the 2D line shape. Rapid fluctuations cause a motionally narrowed homogeneous contribution to the spectrum. On the other hand, slower-evolving molecular environments induce fluctuations in vibrational frequency, leading to inhomogeneous broadening. The microscopic changes in the structural environment result in sampling of the heterogeneous environments and create time dependent stochastic fluctuations in the vibrational frequency, known as spectral diffusion. This phenomenon was characterized by the frequency-frequency correlation function (FFCF).

To analyze the $T_w$ dependent evolution of the 2D IR lineshapes and extract the FFCF, the nodal line slope (NLS) approach was employed [47,50]. This method combined the series of 2D IR spectra into a single decay curve, and the NLS decays were used to calculate the spectral diffusion timescales. The NLS value at $T_w = 0$ ps indicated the degree of homogeneity in the broadening. The NLS decay curves were fitted with a multi-exponential model to extract the time constants, represented by the following equation.

$$C(t) = \sum_{i=1}^{2} a_i e^{\left(\frac{t}{\tau_i}\right)}$$

## 3. Results and discussion

### 3.1. FTIR spectroscopy

The FTIR spectra of the $SCN^-$ (CN stretch) dissolved in two highly viscous solvents (glycerol and malicine) and their respective aqueous mixtures are shown in Fig. 1. Notably, both glycerol and malicine show a

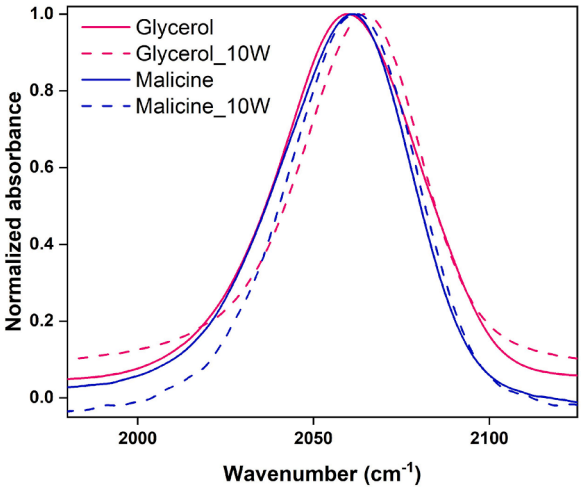


**Fig. 1.** FTIR spectra of $SCN^-$(CN stretch) in solvent Glycerol (solid pink), Glycerol_10W (dashed pink), Malicine (solid blue), and Malicine_10W (dashed blue).

blue shift in the nitrile stretch upon the addition of water. The spectra presented in Fig. 1 exhibit a subtle asymmetry, featuring a small wing on the low-frequency side in each case. Previous studies have attributed such asymmetry to the frequency-dependence of the transition dipole moment in the nitrile stretch within hydrogen bonding environments [47,51,52].

The observed asymmetric lineshapes in glycerol and malicine indicate that the $SCN^-$ anion is already engaged in hydrogen bonding, even in the absence of water. Upon water addition, the extent and strength of these hydrogen bonds increase, leading to the observed blue-shifts in Glycerol_10W and Malicine_10W compared to glycerol and malicine, respectively. The observed blue shift in glycerol (~5 $cm^{-1}$) is larger than that in malicine (1 $cm^{-1}$). Moreover, the peaks appear slightly narrower after water addition (Table 1). This phenomenon may arise from motional narrowing, as non-viscous water molecules exhibit faster fluctuations compared to their viscous counterparts in Malicine_10W and Glycerol_10W.

In addition to motional narrowing, the relative changes in the populations of hydrogen-bonded and non-hydrogen bonded $SCN^-$ species can also influence the full width at half maximum (FWHM) of the peaks. The frequency dependence of the transition dipole moment introduces further complexities to the system. Consequently, the differences in FWHM might not provide highly valuable information. However, the FTIR lineshapes, which are linked to the fluctuation dynamics of the underlying sub-populations, offer the potential for deeper insights into the systems.

### 3.2. 2D IR spectroscopy

2D IR spectroscopy was employed using the $SCN^-$ (CN stretch) as a vibrational probe to investigate the fluctuation dynamics of the solvent systems. A typical 2D IR spectrum consists of a peak pair, where the diagonal peak arises from the 0 → 1 transitions (ground state bleach and stimulated emission), and the other peak, resulting from the 1 → 2 transitions (excited state absorption), is shifted along the detection frequency due to the vibrational anharmonicity of the nitrile stretch. Fig. 2 displays the 2D IR spectra of the nitrile stretch in glycerol and malicine at four different waiting times ($T_w$). At shorter $T_w$ values, the spectra exhibit diagonal elongation as the excitation and detection frequencies show a strong correlation. However, as the solvent structure evolves over time, this correlation gradually diminishes, leading to peak broadening. Notably, Fig. 2 shows that even at larger waiting times, the excitation and detection frequencies remain correlated, indicating that the conformational space is not fully sampled within the experimental time window, constrained by the vibrational lifetime of the nitrile stretch in a specific environment. Surprisingly, among the two viscous solvents, 2D IR peaks in glycerol exhibit a larger elongation than in malicine at any large $T_w$, implying slower inhomogeneous dynamics in glycerol, despite malicine's reported bulk viscosity being higher than that of glycerol.

Fig. 3 shows the 2D IR spectra of Glycerol_10W and Malicine_10W at three different waiting times. As the 2D IR signal is constrained by the vibrational lifetimes ($T_1$), we were unable to study the entire range of waiting times for Glycerol_10W and Malicine_10W, as was done for glycerol and malicine. The presence of water significantly decreases the $T_1$ due to the coupling of the CN vibration with the resonant water mode (bending + libration) through hydrogen bonding interactions (Table 2) [5,53]. A comparison between Figs. 2 and 3 reveals that solvent fluctuations accelerate upon water addition. However, the correlation between excitation and detection frequencies is lost much faster in Glycerol_10W than in Malicine_10W. Interestingly, considering that glycerol exhibits slower dynamics than malicine, it is noteworthy that the addition of water (in the same molar ratio) results in faster fluctuations in the aqueous glycerol solution compared to the aqueous malicine solution. By analyzing the peak shapes, we have quantitatively extracted the underlying fluctuation timescales from the frequency-frequency correlation function (FFCF), which is derived from the 2D IR spectra using the nodal line slope (NLS) method (Table 2) [47,50].

**Table 1**
FTIR lineshape parameters for SCN- (CN stretch) in different solvents and their respective 10W aqueous mixtures.

| Sample | Frequency ($cm^{-1}$) | FWHM ($cm^{-1}$) |
|---|---|---|
| Glycerol | 2059.6 ± 0.2 | 48±1 |
| Glycerol_10W | 2064.9 ± 0.2 | 42±1 |
| Malicine | 2061.1 ± 0.2 | 44±1 |
| Malicine_10W | 2062.1 ± 0.2 | 41±1 |

For all solvation environments, the FFCF could be fitted with bi-exponential decay functions without any offset, indicating the contribution of two distinctly different dynamical processes to the solvation dynamics (Fig. 4). The fast time constants correspond to local solvent fluctuations around the solute, likely arising from solute-solvent hydrogen bond-making and breaking dynamics [36,49]. On the other hand, the slow timescales correspond to the overall evolution of solvent structures. While slow time constants usually follow the trend in bulk viscosity for molecular solvents, DESs are known to form spatially heterogeneous nanodomains [27,28,35,54]. In malicine, due to various types of hydrogen bonding and electrostatic interactions possible, distribution of fluctuation rates may exist, originating from different hydrogen bond dynamics and electrostatic fluctuations. As the slow timescale in malicine arises from the overall evolution of solvent structures across various domains, the variations in dynamics within the different heterogeneous domains may plausibly render the overall dynamics faster than that in a less viscous solvent like glycerol. Additionally, dynamical decoupling has been reported between the solvent and solute motions, particularly in high viscosities [40,55]. A different degree of coupling in the case of homogeneous and heterogeneous viscous solvents may also contribute to slower dynamics in glycerol compared to the DES. A comprehensive understanding can be obtained through molecular dynamics simulations, but this falls outside the scope of our current study.

Upon water addition, the slow time constant in Glycerol_10W decreases nearly threefold compared to Malicine_10W (18.8 ps vs. 58 ps). This result can be understood in the context of spatially heterogeneous domains present in malicine. Water molecules are likely to enter domains where existing interactions can be easily disrupted. Consequently, the stronger the pre-existing interactions, the less likely they are to be disrupted. Malic acid contains two carboxylic acid groups and a hydroxyl moiety, capable of forming strong intermolecular hydrogen bonding interactions with the chloride anion in the DES. A previous NMR spectroscopy study reported that water addition leads to a phase-separated system, with the DES structure preserved and new water-rich domains (aggregates) formed [24]. However, a combined study involving neutron diffraction and molecular dynamics simulations suggested that water is sequestered into the malicine ion structure at a sub-stoichiometric coordination [30]. The remaining water molecules were found to fluxionally occupy interstitial sites that would otherwise not be occupied by larger anions. Thus, the DES structure remains largely intact despite the addition of water.

Table 2 shows that while the amplitude of the faster timescale increases and that of the slower time constant decreases from malicine to Malicine_10W, the slower component still contributes the most to the fluctuation dynamics. This observation further supports the notion that the DES structure is not significantly disrupted by the addition of water.

In contrast, in Glycerol_10W, the amplitude of the faster time constant dominates the dynamics, indicating substantial perturbation of the glycerol hydrogen-bond network by the addition of water. In fact, a recent simulation study on water-glycerol mixtures predicted that water preferentially donates a hydrogen bond to glycerol rather than to another water molecule [33]. On the other hand, glycerol has an equal

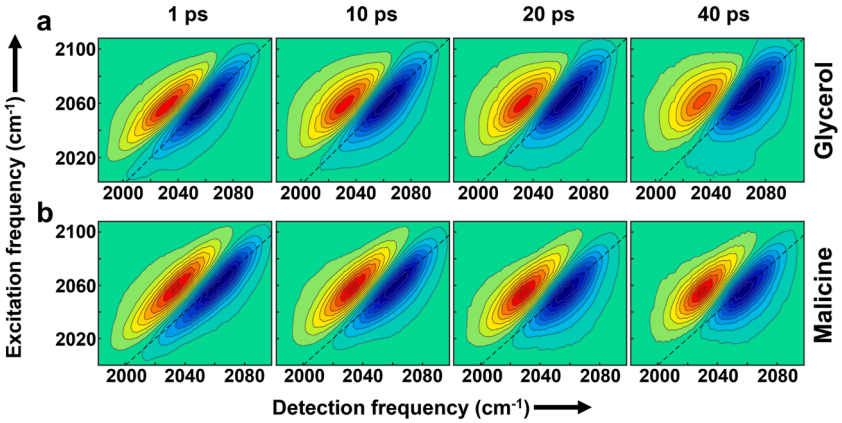


**Fig. 2.** Waiting time ($T_W$) dependent 2D IR spectra for (a) Glycerol and (b) Malicine.

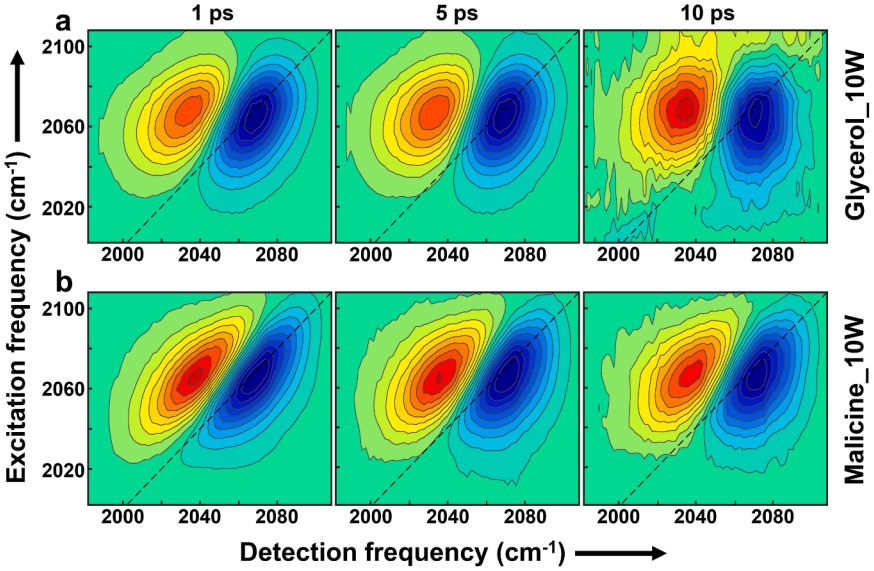


**Fig. 3.** Waiting time ($T_W$) dependent 2D IR spectra for (a) Glycerol_10W and (b) Malicine_10W.

**Table 2**
NLS decay fitting parameters, anharmonicity, and vibrational lifetime parameters.

| Sample | $A_1$ | $\tau_1$ (ps) | $A_2$ | $\tau_2$ (ps) | Anharmonicity ($cm^{-1}$) | $T_1$ (ps) |
|---|---|---|---|---|---|---|
| Glycerol | 0.12 | 3.33±0.62 | 0.77 | 334.00±40.09 | 24.48 | 11.20±0.31 |
| Glycerol_10W | 0.44 | 1.00±0.15 | 0.31 | 18.80±4.33 | 32.99 | 2.32±0.03 |
| Malicine | 0.14 | 1.62±0.26 | 0.76 | 180.00±8.7 | 27.67 | 2.00±0.09, 12.4 ± 0.47 |
| Malicine_10W | 0.21 | 2.80±0.83 | 0.54 | 58.00±20.1 | 30.63 | 2.45±0.05 |

probability of donating a hydrogen bond to either another glycerol molecule or water. As the water content increases, it disrupts the glycerol hydrogen bond network. Our experimental results align with these recently reported simulation findings. Furthermore, previous studies on $SCN^-$ have indicated that hydrogen bonding leads to an increase in the vibrational anharmonicity of the nitrile stretch [5]. The anharmonicity values presented in Table 2 also show that anharmonicity increases upon the addition of water to both glycerol and malicine. Our experimental results show that the anharmonicity increases more drastically upon water addition to glycerol than malicine. It has been previously reported that marked differences in the immediate surroundings of the solute result in different vibrational anharmonicities of $SCN^-$ indicating a more pronounced disruption of the solvation structure [5] when water is added to glycerol compared to malicine. Water disrupts the homogeneous glycerol hydrogen bond network predominantly, while the malicine structure is less affected due to the presence of the spatial heterogeneous network, with water molecules predominantly interacting with the ionic components of the DES or occupying smaller interstitial sites that were previously vacant in the DES. Consequently, the extent of homogeneous and inhomogeneous contributions to the FTIR lineshape is expected to vary to different degrees upon water addition to glycerol and malicine. For a more comprehensive understanding, a detailed study of the inter-component hydrogen bond dynamics in these systems, both with and without the addition of water, would provide valuable molecular insights. However, such an investigation falls beyond the scope of this current work.

## 4. Conclusion

In this study, we have utilized FTIR and 2D IR spectroscopy to gain

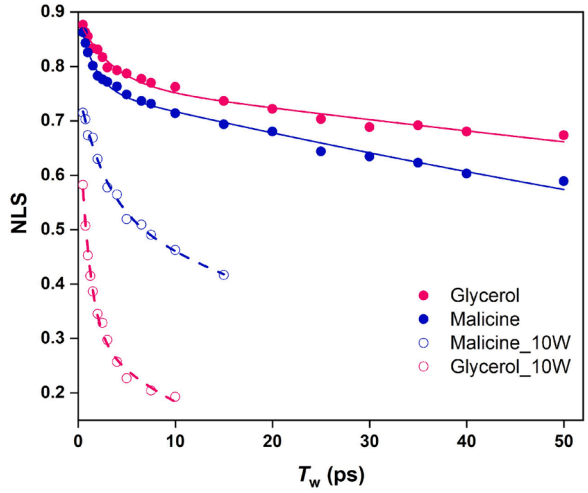


**Fig. 4.** NLS decays measured for $SCN^-$ in Glycerol (solid pink), Malicine (solid blue), Malcine_10W (hollow blue), and Glycerol_10W (hollow pink).

comprehensive insights into the impact of water addition on viscous solvents with varying heterogeneity. Specifically, we investigated two viscous solvents: glycerol, a molecular solvent, and malicine, a DES. Our findings revealed intriguing dynamics in these systems.

Interestingly, despite glycerol having a lower viscosity compared to malicine, the solvent fluctuation dynamics were slower in the molecular liquid. This discrepancy can be attributed to the formation of nanoscale heterogeneous domains in DESs, leading to variations in dynamics within these more or less distinct domains. Consequently, the overall dynamics in DESs may be faster than in less viscous solvents like glycerol.

Furthermore, we explored the effect of water addition to these viscous solvents. The glycerol-water mixture exhibited significantly faster dynamics compared to the malicine-water system. This acceleration in glycerol-water dynamics can be attributed to the complete disruption of the glycerol hydrogen bond network upon water addition. In contrast, previous reports indicate that the DES structure remains intact in the presence of water. This observation is further supported by the relatively slower dynamics in Malicine_10W compared to Glycerol_10W, corroborating previous theoretical findings.

In conclusion, our combined FTIR and 2D IR spectroscopic study sheds light on the complex interplay between water addition and the fluctuation dynamics of viscous solvents with varied heterogeneity, providing valuable insights into the behavior of these systems.

## Research data

Data are available upon reasonable request.

## CRediT authorship contribution statement

**Tubai Chowdhury:** Resources, Formal analysis, Investigation, Methodology, Software. **Sucheta Ghosh:** Formal analysis, Writing – original draft. **Akhil Pathania:** Investigation. **Shivshankar Kore:** Resources, Software. **Akhil B Mon:** Writing – original draft. **Srijan Chatterjee:** Formal analysis. **Samadhan H. Deshmukh:** Writing – original draft. **Sayan Bagchi:** Supervision, Conceptualization, Writing – review & editing.

## Declaration of Competing Interest

The authors declare that they have no known competing financial interests or personal relationships that could have appeared to influence the work reported in this paper.

## Data availability

Data will be made available on request.

## Acknowledgments

SB acknowledges CSIR-NCL and SERB, India (EMR/2016/000576, CRG/2022/004454) for financial support. SK acknowledges DBT, AP acknowledges DST, SG acknowledges IACS for the fellowship, and SHD and TC acknowledge CSIR for research fellowships.

## References

[1] G. Wypych, 13 - solvents use in various industries. Handbook of Solvents, 3rd Edition, ChemTec Publishing, 2019, pp. 901–1124.
[2] P. Deb, T. Haldar, S.M. Kashid, S. Banerjee, S. Chakrabarty, S. Bagchi, Correlating nitrile IR frequencies to local electrostatics quantifies noncovalent interactions of peptides and proteins, J. Phys. Chem. B 120 (2016) 4034–4046.
[3] A. Li, Y. Chen, K. Zhuo, C. Wang, C. Wang, J. Wang, Facile and shape-controlled electrochemical synthesis of gold nanocrystals by changing water contents in deep eutectic solvents and their electrocatalytic activity, RSC Adv. 6 (2016) 8786–8790.
[4] J.A.D. Marquez, M.B.M.Y. Ang, B.T. Doma, S.-H. Huang, H.-A. Tsai, K.-R. Lee, J.-Y. Lai, Application of cosolvent-assisted interfacial polymerization technique to fabricate thin-film composite polyamide pervaporation membranes with PVDF hollow fiber as support, J. Memb. Sci. 564 (2018) 722–731.
[5] S.S. Sakpal, S.H. Deshmukh, S. Chatterjee, D. Ghosh, S. Bagchi, Transition of a deep eutectic solution to aqueous solution: a dynamical perspective of the dissolved solute, J. Phys. Chem. Lett. 12 (2021) 8784–8789.
[6] D. Shah, F.S. Mjalli, Effect of water on the thermo-physical properties of Reline: an experimental and molecular simulation based approach, Phys. Chem. Chem. Phys. 16 (2014) 23900–23907.
[7] S. Sarkar, A. Maity, R. Chakrabarti, Microscopic structural features of water in aqueous–reline mixtures of varying compositions, Phys. Chem. Chem. Phys. 23 (2021) 3779–3793.
[8] A.G.M. Ferreira, A.P.V. Egas, I.M.A. Fonseca, A.C. Costa, D.C. Abreu, L.Q. Lobo, The viscosity of glycerol, J. Chem. Thermodyn. 113 (2017) 162–182.
[9] G. Kowalska, T. Baj, R. Kowalski, J. Szymańska, Optimization of glycerol–water extraction of selected bioactive compounds from peppermint and common nettle, Antioxidants 10 (2021) 817.
[10] E. Basiak, A. Lenart, F. Debeaufort, How glycerol and water contents affect the structural and functional properties of starch-based edible films, Polymers 10 (2018) 412 (Basel).
[11] Y. Xia, Y. Wu, T. Yu, S. Xue, M. Guo, J. Li, Z. Li, Multifunctional glycerol–water hydrogel for biomimetic human skin with resistance memory function, ACS Appl. Mater. Interfaces 11 (2019) 21117–21125.
[12] L.B. Lane, Freezing points of glycerol and its aqueous solutions, Ind. Eng. Chem. 17 (1925) 924. -924.
[13] X. Pan, Q. Wang, D. Ning, L. Dai, K. Liu, Y. Ni, L. Chen, L. Huang, Ultraflexible self-healing guar gum-glycerol hydrogel with injectable, antifreeze, and strain-sensitive properties, ACS Biomater. Sci. Eng. 4 (2018) 3397–3404.
[14] Y. Suzuki, S. Takeya, Slow crystal growth of cubic ice with stacking faults in a glassy dilute glycerol aqueous solution, J. Phys. Chem. Lett. 11 (2020) 9432–9438.
[15] B.B. Hansen, S. Spittle, B. Chen, D. Poe, Y. Zhang, J.M. Klein, A. Horton, L. Adhikari, T. Zelovich, B.W. Doherty, B. Gurkan, E.J. Maginn, A. Ragauskas, M. Dadmun, T.A. Zawodzinski, G.A. Baker, M.E. Tuckerman, R.F. Savinell, J. R. Sangoro, Deep eutectic solvents: a review of fundamentals and applications, Chem. Rev. 121 (2021) 1232–1285.
[16] H.-G. Liao, Y.-X. Jiang, Z.-Y. Zhou, S.-P. Chen, S.-G. Sun, Shape-controlled synthesis of gold nanoparticles in deep eutectic solvents for studies of structure–functionality relationships in electrocatalysis, Angew. Chem. Int. Ed. 47 (2008) 9100–9103.
[17] O. Oderinde, I. Hussain, M. Kang, Y. Wu, K. Mulenga, I. Adebayo, F. Yao, G. Fu, Water as DES-cosolvent on the morphology tuning and photochromic enhancement of tungsten oxide-molybdenum oxide nanocomposite, J. Ind. Eng. Chem. 80 (2019) 1–10.
[18] C.R. Ashworth, R.P. Matthews, T. Welton, P.A. Hunt, Doubly ionic hydrogen bond interactions within the choline chloride–urea deep eutectic solvent, Phys. Chem. Chem. Phys. 18 (2016) 18145–18160.
[19] V. Alizadeh, D. Geller, F. Malberg, P.B. Sánchez, A. Padua, B. Kirchner, Strong microheterogeneity in novel deep eutectic solvents, ChemPhysChem 20 (2019) 1786–1792.
[20] C. Florindo, F.S. Oliveira, L.P.N. Rebelo, A.M. Fernandes, I.M. Marrucho, Insights into the synthesis and properties of deep eutectic solvents based on cholinium chloride and carboxylic acids, ACS Sustain. Chem. Eng. 2 (2014) 2416–2425.
[21] O.S. Hammond, D.T. Bowron, K.J. Edler, The effect of water upon deep eutectic solvent nanostructure: an unusual transition from ionic mixture to aqueous solution, Angew. Chem. Int. Ed. 56 (2017) 9782–9785.
[22] C. D'Agostino, R.C. Harris, A.P. Abbott, L.F. Gladden, M.D. Mantle, Molecular motion and ion diffusion in choline chloride based deep eutectic solvents studied by $^1$H pulsed field gradient NMR spectroscopy, Phys. Chem. Chem. Phys. 13 (2011) 21383–21391.

[23] T. Zhekenov, N. Toksanbayev, Z. Kazakbayeva, D. Shah, F.S. Mjalli, Formation of type III deep eutectic solvents and effect of water on their intermolecular interactions, Fluid Phase Equilib. 441 (2017) 43–48.
[24] C. D'Agostino, L.F. Gladden, M.D. Mantle, A.P. Abbott, I.A. Essa, A.Y. Al-Murshedi, R.C. Harris, Molecular and ionic diffusion in aqueous–deep eutectic solvent mixtures: probing inter-molecular interactions using PFG NMR, Phys. Chem. Chem. Phys. 17 (23) (2015) 15297–15304.
[25] S. Chatterjee, S.H. Deshmukh, S. Bagchi, Does viscosity drive the dynamics in an alcohol-based deep eutectic solvent? J. Phys. Chem. B 126 (2022) 8331–8337.
[26] S. Kaur, A. Gupta, H.K. Kashyap, How hydration affects the microscopic structural morphology in a deep eutectic solvent, J. Phys. Chem. B 124 (2020) 2230–2237.
[27] S. Kaur, A. Gupta, H.K. Kashyap, Nanoscale spatial heterogeneity in deep eutectic solvents, J. Phys. Chem. B 120 (2016) 6712–6720.
[28] S. Chatterjee, T. Haldar, D. Ghosh, S. Bagchi, Electrostatic manifestation of micro-heterogeneous solvation structures in deep-eutectic solvents: a spectroscopic approach, J. Phys. Chem. B 124 (2020) 3709–3715.
[29] S. Spittle, D. Poe, B. Doherty, C. Kolodziej, L. Heroux, M.A. Haque, H. Squire, T. Cosby, Y. Zhang, C. Fraenza, S. Bhattacharyya, M. Tyagi, J. Peng, R. A. Elgammal, T. Zawodzinski, M. Tuckerman, S. Greenbaum, B. Gurkan, C. Burda, M. Dadmun, E.J. Maginn, J. Sangoro, Evolution of microscopic heterogeneity and dynamics in choline chloride-based deep eutectic solvents, Nat. Commun. 13 (2022) 219.
[30] O.S. Hammond, D.T. Bowron, A.J. Jackson, T. Arnold, A. Sanchez-Fernandez, N. Tsapatsaris, V. Garcia Sakai, K.J. Edler, Resilience of malic acid natural deep eutectic solvent nanostructure to solidification and hydration, J. Phys. Chem. B 121 (2017) 7473–7483.
[31] V. Alizadeh, F. Malberg, A.A.H. Pádua, B. Kirchner, Are there magic compositions in deep eutectic solvents? Effects of composition and water content in choline chloride/ethylene glycol from *ab initio* molecular dynamics, J. Phys. Chem. B 124 (2020) 7433–7443.
[32] B. Liu, J. Zhao, F. Wei, Effects of water on the properties of acetamide-KSCN eutectic ionic liquids at several temperatures, J. Mol. Liq. 187 (2013) 309–313.
[33] T.R. Fisher, G. Zhou, Y. Shi, L. Huang, How does hydrogen bond network analysis reveal the golden ratio of water–glycerol mixtures? Phys. Chem. Chem. Phys. 22 (2020) 2887–2907.
[34] A.R. Harifi-Mood, R. Buchner, Density, viscosity, and conductivity of choline chloride+ethylene glycol as a deep eutectic solvent and its binary mixtures with dimethyl sulfoxide, J. Mol. Liq. 225 (2017) 689–695.
[35] T. Pal, R. Biswas, Heterogeneity and viscosity decoupling in (acetamide+ electrolyte) molten mixtures: a model simulation study, Chem. Phys. Lett. 517 (2011) 180–185.
[36] Y. Cui, K.D. Fulfer, J. Ma, T.K. Weldeghiorghis, D.G. Kuroda, Solvation dynamics of an ionic probe in choline chloride-based deep eutectic solvents, Phys. Chem. Chem. Phys. 18 (2016) 31471–31479.
[37] Y. Cui, J.C. Rushing, S. Seifert, N.M. Bedford, D.G. Kuroda, Molecularly heterogeneous structure of a nonionic deep eutectic solvent composed of N-methylacetamide and lauric acid, J. Phys. Chem. B 123 (2019) 3984–3993.
[38] A. Tamimi, H.E. Bailey, M.D. Fayer, Alkyl chain length dependence of the dynamics and structure in the ionic regions of room-temperature ionic liquids, J. Phys. Chem. B 120 (2016) 7488–7501.
[39] M.D. Fayer, Dynamics and structure of room temperature ionic liquids, Chem. Phys. Lett. 616–617 (2014) 259–274.
[40] S.A. Yamada, H.E. Bailey, A. Tamimi, C. Li, M.D. Fayer, Dynamics in a room-temperature ionic liquid from the cation perspective: 2D IR vibrational echo spectroscopy, J. Am. Chem. Soc. 139 (2017) 2408–2420.
[41] C.H. Giammanco, P.L. Kramer, D.B. Wong, M.D. Fayer, Water dynamics in 1-alkyl-3-methylimidazolium tetrafluoroborate ionic liquids, J. Phys. Chem. B 120 (2016) 11523–11538.
[42] P.L. Kramer, C.H. Giammanco, M.D. Fayer, Dynamics of water, methanol, and ethanol in a room temperature ionic liquid, J. Chem. Phys. 142 (2015).
[43] H. Bian, H. Chen, Q. Zhang, J. Li, X. Wen, W. Zhuang, J. Zheng, Cation effects on rotational dynamics of anions and water molecules in alkali ($Li^+$, $Na^+$, $K^+$, $Cs^+$) thiocyanate ($SCN^-$) aqueous solutions, J. Phys. Chem. B 117 (2013) 7972–7984.
[44] K.-I. Oh, J.-H. Choi, J.-H. Lee, J.-B. Han, H. Lee, M. Cho, Nitrile and thiocyanate IR probes: molecular dynamics simulation studies, J. Chem. Phys. 128 (15) (2008).
[45] Z. Ren, T. Brinzer, S. Dutta, S. Garrett-Roe, Thiocyanate as a local probe of ultrafast structure and dynamics in imidazolium-based ionic liquids: water-induced heterogeneity and cation-induced ion pairing, J. Phys. Chem. B 119 (2015) 4699–4712.
[46] S.H. Deshmukh, S. Chatterjee, D. Ghosh, S. Bagchi, Ligand dynamics time scales identify the surface–ligand interactions in thiocyanate-capped cadmium sulfide nanocrystals, J. Phys. Chem. Lett. 13 (2022) 3059–3065.
[47] S. Kore, R.R. Sahoo, B. Santra, A. Sarkar, T. Chowdhury, S.H. Deshmukh, S. Hazarika, S. Chatterjee, S. Bagchi, Solvation structure and dynamics of a small ion in an organic electrolyte, J. Photochem. 440 (2023), 114666.
[48] A.P. Abbott, D. Boothby, G. Capper, D.L. Davies, R.K. Rasheed, Deep eutectic solvents formed between choline chloride and carboxylic acids: versatile alternatives to ionic liquids, J. Am. Chem. Soc. 126 (2004) 9142–9147.
[49] S. Chatterjee, D. Ghosh, T. Haldar, P. Deb, S.S. Sakpal, S.H. Deshmukh, S. M. Kashid, S. Bagchi, Hydrocarbon chain-length dependence of solvation dynamics in alcohol-based deep eutectic solvents: a two-dimensional infrared spectroscopic investigation, J. Phys. Chem. B 123 (2019) 9355–9363.
[50] Z.A. Al-Mualem, C.R. Baiz, Generative adversarial neural networks for denoising coherent multidimensional spectra, J. Phys. Chem. A 126 (2022) 3816–3825.
[51] J.P. Breen, L.C. Leibfried, X. Xing, M.D. Fayer, Long-range interface effects in room temperature ionic liquids: vibrational lifetime studies of thin films, J. Phys. Chem. B 127 (2023) 6217–6226.
[52] M. Okuda, K. Ohta, K. Tominaga, Comparison of vibrational dynamics between non-ionic and ionic vibrational probes in water: experimental study with two-dimensional infrared and infrared pump-probe spectroscopies, J. Chem. Phys. 145 (2016).
[53] P. Hamm, M. Lim, R.M. Hochstrasser, Vibrational energy relaxation of the cyanide ion in water, J. Chem. Phys. 107 (1997) 10523–10531.
[54] S. Chatterjee, T. Chowdhury, S. Bagchi, Does variation in composition affect dynamics when approaching the eutectic composition? J. Chem. Phys. 158 (2023), 114203.
[55] P.L. Kramer, J. Nishida, C.H. Giammanco, A. Tamimi, M.D. Fayer, Observation and theory of reorientation-induced spectral diffusion in polarization-selective 2D IR spectroscopy, J. Chem. Phys. 142 (2015), 184505.